Light-Assisted Synthesis of Pt−Zn Porphyrin Nanocomposites and Their Use for Electrochemical Detection of Organohalides

Wisitsree Wiyaratn,[†,‡] Sabahudin Hrapovic,[†] Yali Liu,[†] Werasak Surareungchai,[§] and John H. T. Luong*,[†]

Biotechnology Research Institute, National Research Council Canada (NRCC), Montreal, Quebec, Canada, H4P 2R2, The Joint Graduate School of Energy and Environment. Division of Environment, King Mongkut's University Technology Thonburi, Toong-kru, Bangkok, Thailand, and Division of Biotechnology, School of Bioresources and Technology, King Mongkut's University Technology Thonburi, Thakam, Bangkok, Thailand

Pt−Zn porphyrin nanocomposites have been synthesized using zinc porphyrin and dihydrogen hexachloroplatinate in the presence of light and ascorbic acid. TEM and AFM imaging revealed that Pt nanoparticles with an average diameter of ∼3.5 nm were embedded within the Zn porphyrin matrix. The glassy carbon electrode was modified with Nafion-stabilized Pt−Zn porphyrin nanocomposites and used for dehalogenation of carbon tetrachloride, chloroform, pentachlorophenol, chlorobenzene, and hexachlorobenzene as five test models. The Pt−Zn porphyrin nanocomposite-modified electrode exhibited catalytic activity for the reduction of organohalides at −1.0 V versus Ag/AgCl. Raman signatures confirmed the dehalogenation of chlorobenzene by the nanocomposite-modified electrode. The above two aliphatic and three aromatic organohalides had detection limits of 0.5 μM with linearity up to 8 μM. The modified electrode was good for at least 80 repeated measurements of 4 μM chlorobenzene with a storage stability of 1 month at room temperature. The deactivation of the electrode activity was associated with the loss of platinum nanoparticles from the nanocomposite structure.

The halogenated hydrocarbons or organohalides, mainly chlorinated compounds, have been widely used as industrial solvents and biocides in agricultural or domestic uses. They are one of the largest groups of environmental pollutants with significant health concerns such as cancer, deformity, and health disorders even at low levels. In 1970, trichloromethane and short-chain halogenated hydrocarbons were first identified in drinking water. Since then, such dangerous compounds have been included in the Toxic Pollutant List of the U.S. Environmental Protection Agency (EPA). Hence, the determination of organohalides at trace levels has become an important subject in analytical, environmental, and clinical chemistry. Selective and sensitive analysis of organohalides has focused on liquid chromatography and gas chromatography equipped with mass spectrometry. Although universal, such analytical procedures are generally not suitable for rapid on-site or large area monitoring programs owing to the requirement of expensive instrumentation and time-consuming sample preparation. Consequently, there is a critical need for the development of inexpensive analytical systems that enable the rapid and sensitive estimation of organohalides.[1,2]

Electrochemical detection by reductive dehalogenation has been performed using transition-metal coenzymes,[1,2] vitamin B12,[3] coenzyme F430 (a nickel tetrapyrrole-hydrocorphin, found in methyl coenzyme M reductase, the enzyme that catalyzes the final stages of the reduction of carbon dioxide to methane in methanogenic bacteria),[1,2] hemoglobin,[4] and myoglobin.[4,5] Besides its instability, the retention of such a mediator on the active surface of the electrode is always problematical. Although organohalides can be reduced at metal electrodes such as Hg, GC, Pt, or Zn, the required potential is extreme, −1.3 to −2.4 V versus SCE.[6−10] Under such operating conditions, hydrogen evolution occurs and renders the organohalide reaction inefficient, due to the formation of bubbles on the electrode surface. The electrochemical reduction at a Zn/PTFE composite-plated electrode for the chronocoulometric determination of some selected organohalides was attempted.[11] Because of hydrophobicity of the coating, water

* Corresponding author. Fax: 514-496-6265. Tel: 514-496-6175. E-mail: john.luong@cnrc-nrc.gc.ca.

† National Research Council Canada.

‡ The Joint Graduate School of Energy and Environment. Division of Environment, King Mongkut's University Technology Thonburi.

§ Division of Biotechnology, School of Bioresources and Technology, King Mongkut's University Technology Thonburi.

(1) (a) Peter, J.; Hutter, W.; Hampel, W. *Biosens. Bioelectron.* **1996**, *11*, 1215. (b) Hutter, W.; Peter, J.; Swoboda, H.; Hampel, W.; Rosenberg, E.; Kramer, D.; Kellner, R. *Anal. Chim. Acta* **1995**, *306*, 237.

(2) Peter, J.; Hutter, W.; Stollnberger, W.; Karner, F.; Hampel, W. *Anal. Chem.* **1997**, *69*, 2077.

(3) Lexa, D.; Saveant, J. M.; Su, K. B.; Wang, D. L. *J. Am. Chem. Soc.* **1987**, *109*, 6464.

(4) Wright, M.; Honeychurch, M. J.; Hill, H. A. O. *Electrochem. Commun.* **1999**, *1*, 609.

(5) Ordaz, A. A.; Bedioui, F. *Sens. Actuators, B* **1999**, *59*, 128.

(6) Merica, S. G.; Bunce, N. J.; Jedral, W.; Lipkowski, J. *J. Appl. Electrochem.* **1998**, *28*, 645.

(7) Mubarak, M. S.; Peters, D G. *J. Electroanal Chem.* **2001**, *507*, 110.

(8) Greef, R.; Peat, R.; Peter, L. M.; Pletcher, D.; Robinson, J. *Instrumental Methods in Electrochemistry;* Kemp, T. J., Ed.; Ellis Horwood Series in Physical Chemistry; E. Horwood: Chichester, England, 1993; p 16.

(9) Lin, C. H.; Tseng, S. K. *Chemosphere* **2002**, *39*, 2375.

(10) (a) Dahm, C. E.; Peters, D. G. *Anal. Chem.* **1994**, *66*, 3117. (b) Tokoro, R.; Bilewicz, R.; Osteryoung, J. *Anal. Chem.* **1986**, *58*, 1964.

10.1021/ac0509612 CCC: $30.25
Published on Web 00/00/0000

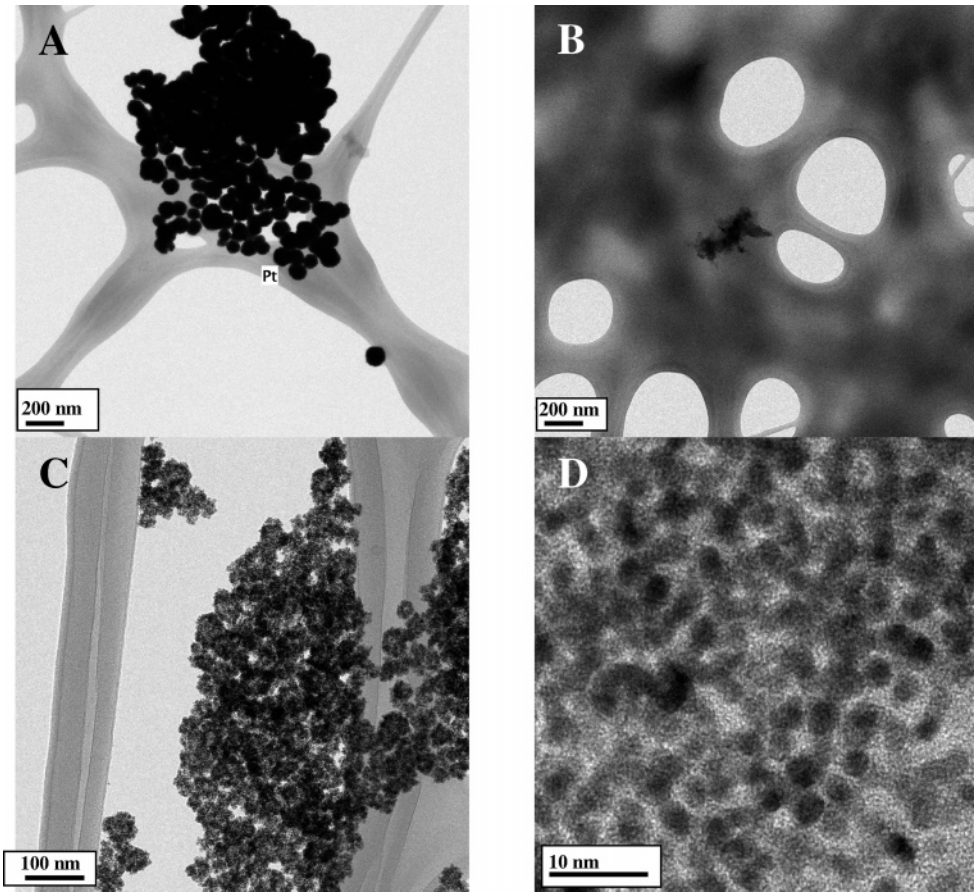

Figure 1. TEM images of Pt nanoparticles prepared by ascorbic acid-assisted chemical reduction of H_2PtCl_6 (A). Formation of Pt nanoparticles was prevented by adding Zn porphyrin in the mixture of H_2PtCl_6 and ascorbic acid and keeping the sample in the dark (B). Preparation of Pt−Zn porphyrin nanocomposites occurs when the solution of Zn porphyrin, H_2PtCl_6, and ascorbic acid is irradiated with light (C). Image D, same as (C) but under higher magnification, showing the 3.5-nm Pt nanoparticles embedded in Zn porphyrin.

molecules are expelled from the electrode surface, and therefore, hydrogen evolution is greatly suppressed. However, this method only provided detection limits of 50 μM and is vulnerable to interference from other organic reduction. Improved selectivity and detection limit can be realized by using the Zn/PTFE composite-plated electrode to catalyze the organohalide sample with the resulting halide ions detected at an Ag electrode by stripping voltammetry.[12] However, because of the detection potential (−1.8 V), this sensor was not very stable. To date, electrochemical analysis of organohalides has focused on redox catalysis using electrodes modified by metal complexes.[13−16] Metal complexes, Fe, Ni, and particularly Co porphyrins, corrins, and phthalocyanines, as well as some other metals and ligands can catalyze organohalides via the reduction of the central metal at moderate potentials:[13]

$$RX + H^+ + 2e^- \rightarrow RH + X^-$$

where RX = organohalides, RH = product, and X^- = halide ion.

Detection limits reported so far range from 0.5 to 30 μM for a variety of organohalides using cobalt(II) tetraphenylporphine,[14] 0.5 to 4 μM (60−1200 ppb) for four different organochlorides and bromides using electropolymerized cobalt porphyrin and salen films,[15] and 80 μM for 3,4-dichloropropylanilide using iron(III) porphyrin.[16]

Nanoparticles fabricated from metals and metal oxides are capable of increasing the activities for many chemical reactions due to the high ratio of surface atoms with free valence to the cluster of total atoms. Besides large surface area-to-volume ratio for the nanoparticle-derivatized materials, the size controllability, chemical stability, and surface tenability provide an ideal platform for exploiting such nanostructures in sensing and catalytic applications. Few reports have resulted in synthesizing such an organic molecule of porphyrins at the nanoscale to enhance photosensitivity for high photoconductive devices or organic solar cells.[17−19] Porphyrin nanostructures are promising components of advanced materials because of their rich photochemistry and efficient catalytic activity.

(11) Wiyaratn, W.; Somasundrum, M.; Surareungchai, W. *Electroanalysis* **2003**, *15*, 1791.
(12) Wiyaratn, W.; Somasundrum, M.; Surareungchai, W. *Anal. Chem.* **2004**, *76*, 2266.
(13) Kashiwagi, Y.; Kikuchi, C.; Anzai, J.-I. *J. Electroanal. Chem.* **2002**, *518*, 51.
(14) Dobson, D. J.; Saini, S. *Anal. Chem.* **1997**, *69*, 3532.
(15) Ordaz, A. A.; Rocha, M. J.; Aguilar, A. J.; Granados, G. G.; Bedioui, F. *Analusis* **2000**, *28*, 238.
(16) Priyantha, N.; Weerabahu, D. *Anal. Chim. Acta* **1996**, *320*, 263.
(17) Gong, X.; Milic, T.; Xu, C.; Batteas, D. J.; Drain, M. C. *J. Am. Chem. Soc.* **2002**, *124*, 14290.
(18) Yang, Z.; Chen, H.; Cao, L.; Li, H.; Wang, M. *Mater. Lett.* **2004**, *58*, 2238.
(19) Nitschke, C.; O'Flaherty, S. M.; Kroll, M.; Blau, J. W. *J. Phys. Chem. B* **2004**, *108*, 1287.

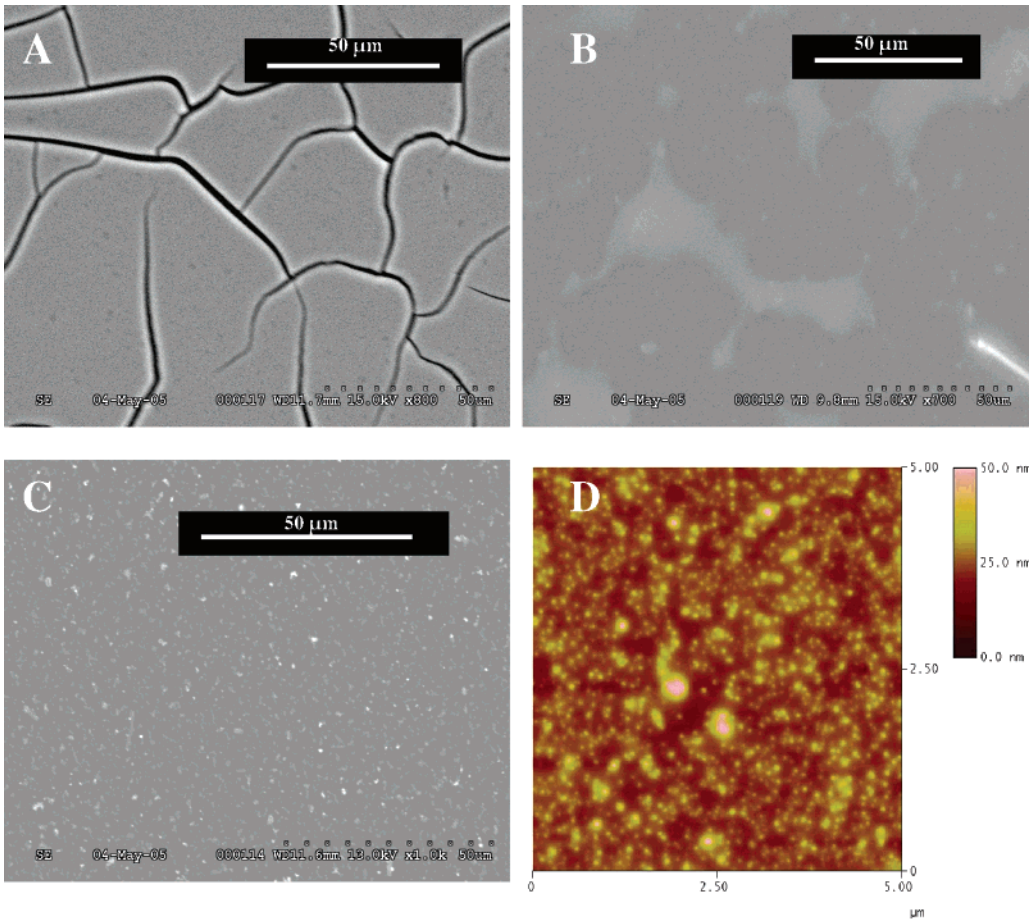

Figure 2. SEM micrographs of GC electrodes modified with Zn porphyrin and Nafion (×800) (A). Solution of Zn porphyrin, H_2PtCl_6, and ascorbic acid keeping the sample in the dark (×700) (B). Pt−Zn porphyrin nanocomposites made from Zn porphyrin, H_2PtCl_6, and ascorbic acid with light exposure (×1000) (C). AFM (tapping mode with a Si tip) (5 μm × 5 μm) of GC electrode modified with Pt−Zn porphyrin nanocomposites (D).

In this study, we report on a novel procedure for synthesis and characterization of platinum−porphyrin composites and explore the assembly of such nanostructures as sensing materials for analysis of organohalides. We anticipate that this might enhance the signal response toward the catalysis of electrochemical reduction of organohalides at lower overpotentials with better sensitivity and reproducibility.

EXPERIMENTAL SECTION

Materials. Analytical grade carbon tetrachloride, chloroform, pentachlorophenol, chlorobenzene, hexachlorobenzene, acetonitrile, dimethylformamide, zinc 5,10,15,20,-tetra(4-pyridyl)-21*H*,23*H*-porphine tetrakis(methochloride) (ZnTPP), ascorbic acid, tetrabutylammonium perchlorate (TBAP, electrochemical grade), and Nafion-perfluorinated ion-exchange resin (5 wt %) were obtained from Aldrich-Sigma (St. Louis, MO). Dihydrogen hexachloroplatinate was a product of Alfa Aesar (Ward Hill, MA).

Instrumentation. For transmission electron microscope (TEM) imaging, a drop of the Pt−Zn porphyrin nanocomposite suspension was dropped on a holey carbon film, 300-mesh copper grid and allowed to dry in air. TEM data were recorded by a Philips CM20 200 kV electron microscope equipped with an Oxford Instruments energy-dispersive X-ray diffraction spectrometer (Link exl II) and an UltraScan 1000 CCD camera. Modified GC electrodes (3 mm in diameter) were prepared by dropping 8 μL of the pertinent solution on the electrode surface and drying in air. Scanning electron microscopy (SEM) analysis was performed directly on modified glassy carbon electrodes using a Hitachi (Tokyo, Japan) S-2600N scanning electron microscope. Scanning probe microscope (Nanoscope IV, Digital Instruments-Veeco, Santa Barbara, CA), with a silicon tip was operated in tapping mode to characterize the surface morphology of GC electrodes modified by the Pt−Zn porphyrin nanocomposite. UV/visible measurements were performed using a Beckman spectrophotometer (DU 640, Fullerton, CA). Fluorescence was measured by a Gilford Fluoro IV spectrofluorometer (Gilford, Oberlin, OH). Raman signatures of liquid samples were obtained by a Horiba/Jobin Yvon laser Raman analyzer LabRAM HR 800 (Horiba/Jobin Yvon, Longjumeau, France) equipped with a frequency-doubled Nd:YAG 532.1-nm laser operating at 30 mW of power. Cyclic voltammetry (CV), and amperometric measurements were performed using an electrochemical analyzer coupled with a picoampere booster and Faraday cage (CHI 601A, CH Instruments, Austin, TX). A Pt wire (Aldrich, 99.9% purity, 1-mm diameter) and an Ag/AgCl, 3 M NaCl (BAS, West Lafayette, IN) electrode were used as counter and reference electrodes, respectively. An Oriel arc lamp source (Newport Oriel Instruments, Irvine, CA) with an Osram XBO 150-W xenon lamp was used for the preparation of Pt −Zn porphyrin nanocomposites. The light was irradiated through a 1.5-in. light condenser without any filter. The light

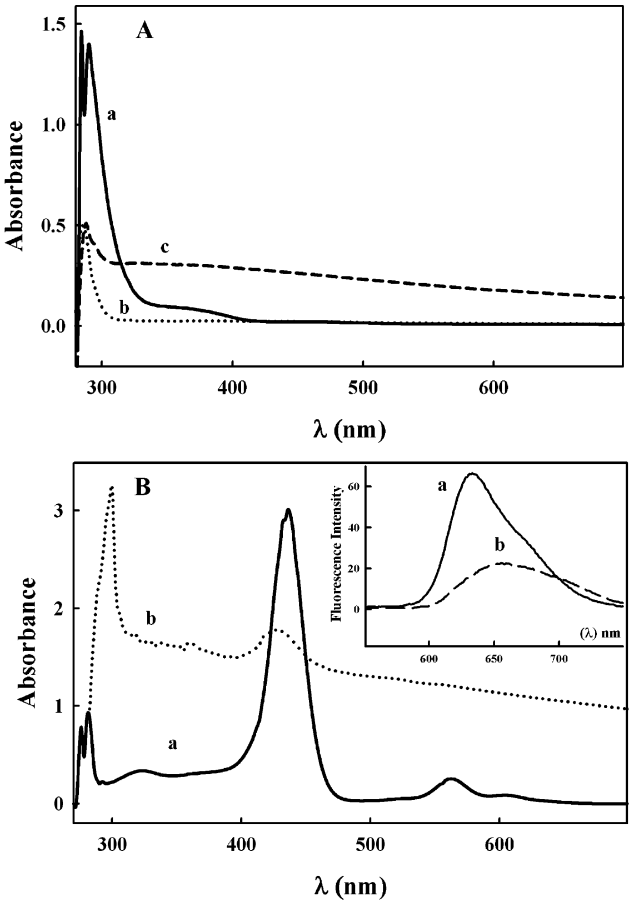

Figure 3. (A) UV−visible spectra of Pt nanoparticles with ascorbic acid only: 0 min (a), 10 min H_2PtCl_6 reduction (b), and 20 min (c). (B) Light-assisted Pt−Zn porphyrin nanocomposite formation from Zn porphyrin, H_2PtCl_6, and ascorbic acid. The inset shows fluorescence emission spectra (excitation 400 nm) of solutions of Zn porphyrin, H_2PtCl_6, and ascorbic acid: without (a) and with (b) light irradiation.

intensity was measured with a Melles Griot handheld power meter 18 LAB 250 (Melles Griot Optics, Irvine, CA).

Electrode Preparation. Glassy carbon electrodes (3 mm in diameter, BAS) were polished with polishing paper (grid 2000) and subsequently with alumina until a mirror finish was obtained. After 5 min of sonication to remove the alumina residues, the electrodes were immersed in concentrated H_2SO_4 for 3 min followed by thorough rinsing with water and ethanol. The electrodes were transferred to the electrochemical cell for cleaning by cyclic voltammetry between −0.5 and +1.2 V versus Ag/AgCl at 100 mV s^{-1} until stable CV profiles were obtained. For the activation of the electrode surface as well as the improvement of Pt nanoparticle adhesion on the GC electrode surface, the cycling was terminated by stepping the potential to +1.2 V for 2 min.[21] The resulting electrodes were dried under a nitrogen stream and used immediately for modification. The Pt−Zn porphyrin nanocomposites (4 μL) were dropped on the active electrode surface and dried at room temperature followed by the application of two Nafion layers (4 μL each).

(20) Song, Y.; Yang, Y.; Medforth, C. J.; Pereira, E.; Singh, A. K.; Xu, H.; Jiang, Y.; Brinker, C. J.; van Swol, F.; Shelnutt, J. A. *J. Am. Chem. Soc.* **2004**, *126*, 635.

(21) Hrapovic, S.; Liu Y.; Male, K. B.; Luong, J. H. T. *Anal. Chem.* **2004**, *76*, 1083.

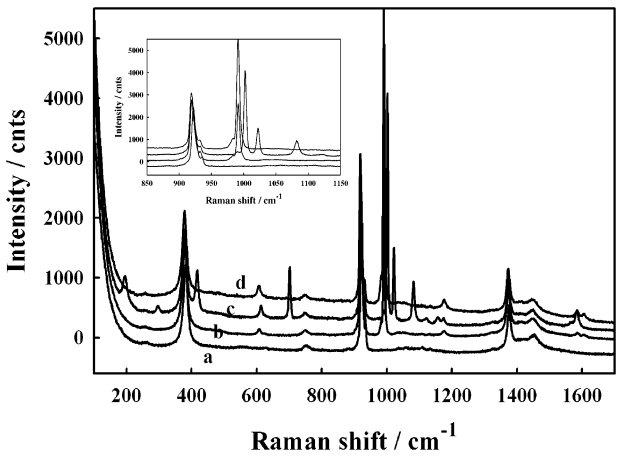

Figure 4. Raman spectroscopy of 0.1 M TBAP/ACN solution as background (a), benzene (b), chlorobenzene (c), and the product of reduction of chlorobenzene (d) upon 50 consecutive cyclic CVs (from 0 to −1.4 V vs Ag/AgCl) at a scan rate 0.05 V/s. The starting chlorobenzene and benzene concentrations were 2 mM in 0.1 M TBAP/ACN solution.

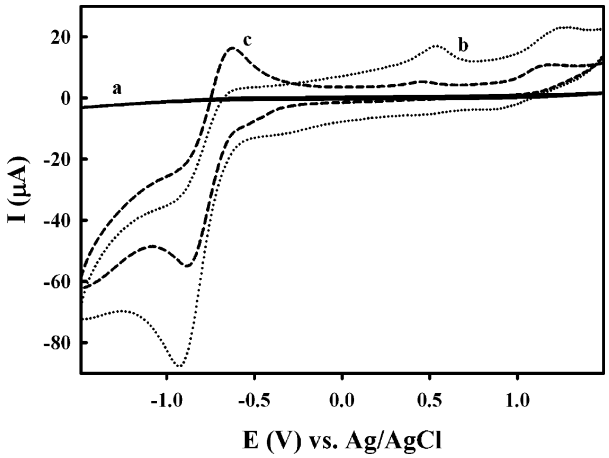

Figure 5. Cyclic voltammograms (wide range) in 0.1 M TBAP/ACN solution at a scan rate 0.05 V/s of (a) bare GC modified with Nafion, (b) GC modified with Zn porphyrin and Nafion, and (c) GC modified with Pt−Zn porphyrin nanocomposites and Nafion.

Table 1. Redox Potentials of Zn Porphyrin/GC/Nafion and Pt−Zn Porphyrin/GC/Nafion Nanocomposite in Acetonitrile with 0.1 M Tetrabutylammonium Perchlorate as the Supporting Electrolyte

redox system	ZnP/GC/Nafion $E_{1/2}$ (V) vs Ag/AgCl	Pt_{nano}−ZnP/GC/Nafion $E_{1/2}$ (V) vs Ag/AgCl	$E_{1/2}$ (V) vs SCE[22]
$[ZnP]/[ZnP]^{+\bullet}$	0.505	0.445[a]	0.890
$[ZnP]^{+\bullet}/[ZnP]^{2+}$	1.065	1.085[a]	1.210
$[ZnP]/[ZnP]^{-}$	−0.920[b]	−0.750	−1.290

[a] E_{pa}. [b] E_{pc}.

Synthesis of Pt−Zn Porphyrin Nanocomposites. Dihydrogen hexachloroplatinate (60 mM), Zn porphyrin (1.5 mM), and ascorbic acid (1 M) were used as three stock solutions for the Pt−Zn porphyrin nanocomposite preparation. A 1-mL sample of Zn porphyrin stock solution was mixed with 9 mL of water.

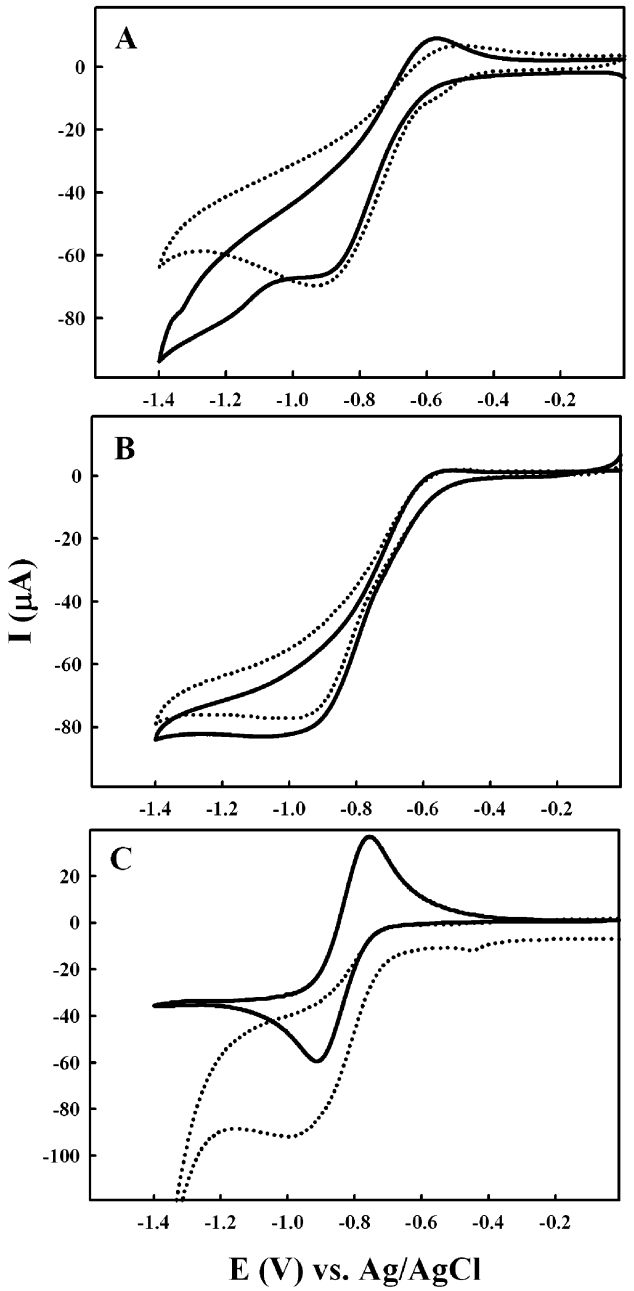

Figure 6. Cyclic voltammetry response of the modified glassy carbon electrodes in 0.1 M TBAP/ACN solution at scan rate 0.05 V/s before (dotted line) and after (line) additions of $CHCl_3$ (2 mM): (A) modified with Zn porphyrin and Nafion, (B) modified with Zn porphyrin, H_2PtCl_6, ascorbic acid and Nafion (dark conditions), and (C) modified with Pt−Zn porphyrin nanocomposites and Nafion (light-irradiated Zn porphyrin, H_2PtCl_6, and ascorbic acid).

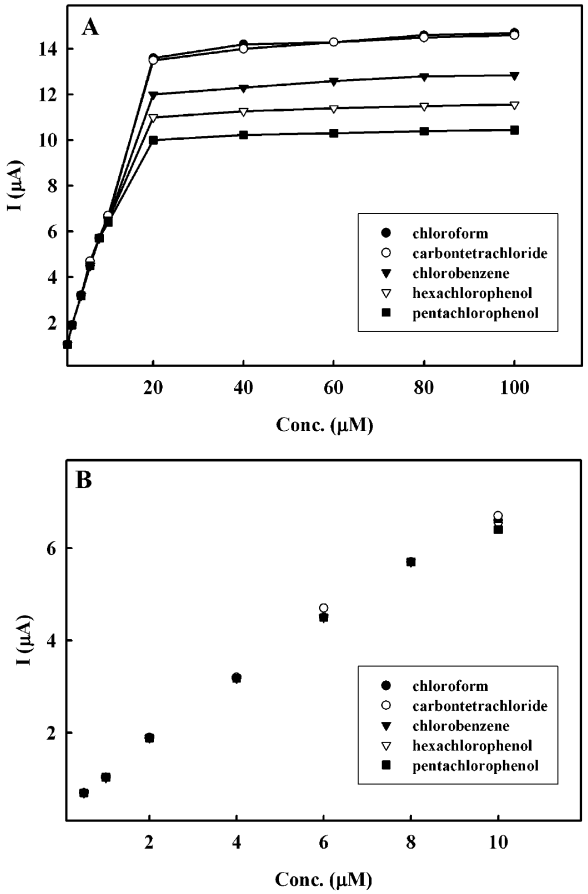

Figure 7. (A) Amperometric current response vs concentration for chloroform, carbon tetrachloride, hexachlorobenzene, chlorobenzene, and pentachlorophenol at −1.0 V vs Ag/AgCl in 0.1 M TBAP/ACN. (B) Calibration curves showing linear range (from 0.5 to 10 μM) for chloroform, carbon tetrachloride, hexachlorobenzene, chlorobenzene, and pentachlorophenol detected amperometrically at −1.0 V, using a Pt−Zn porphyrin nanocomposite in 0.1 M TBAP/ACN.

Ascorbic acid (20 μL) was added to the mixture, followed by 50 μL of dihydrogen hexachloroplatinate stock solution. After mixing, the starting color of the solution was dark yellow, an inherent property of the Pt salt. The resulting solution (10 mL) was exposed to the xenon light source with an intensity of 890 mW for 10 min. The reaction chamber was positioned 15 cm from the light condenser to minimize heating effects. Upon irradiation with light, the photocatalysis reaction started and the color changed to dark red due to the presence of Zn porphyrin in the solution. The color intensified with increasing irradiation time, and the reaction was completed after 10 min with a resulting dark brown-black. Without light irradiation, the resulting solution was only slightly darker (even after a few hours) compared to the starting color (dark yellow), indicating that the Pt−Zn porphyrin nanocomposite formation did not occur. For comparison, the reduction of platinum salt was also studied without Zn porphyrin. Although the reaction occurred also in minutes, the resulting solution was almost black and precipitated after 10−15 min. The reaction was somewhat specific to dihydrogen hexachloroplatinate since no composites were formed when tetrachloroaurate(III) was used in the synthesis.

Mechanism of the Nanocomposite Growth. The formation of Pt−Zn porphyrin nanocomposites is based on the combination of chemical seeding of Pt nanoparticles followed by their photocatalytic growth and interactions with Zn porphyrin. Basically, the slow chemical reduction of H_2PtCl_6 by ascorbic acid occurs to give Pt nanoparticle seeds by the redox reaction:[20]

$$Pt^{2+} + AA \rightarrow Pt^{o} + AA_{ox}$$

The photocatalytic reduction of platinum salt by zinc, occurred in the presence of light and an electron donor (ED) or ascorbic acid in this study. The porphyrin photoreaction is a reductive photocatalytic cycle, which has been used previously in the photosyn-

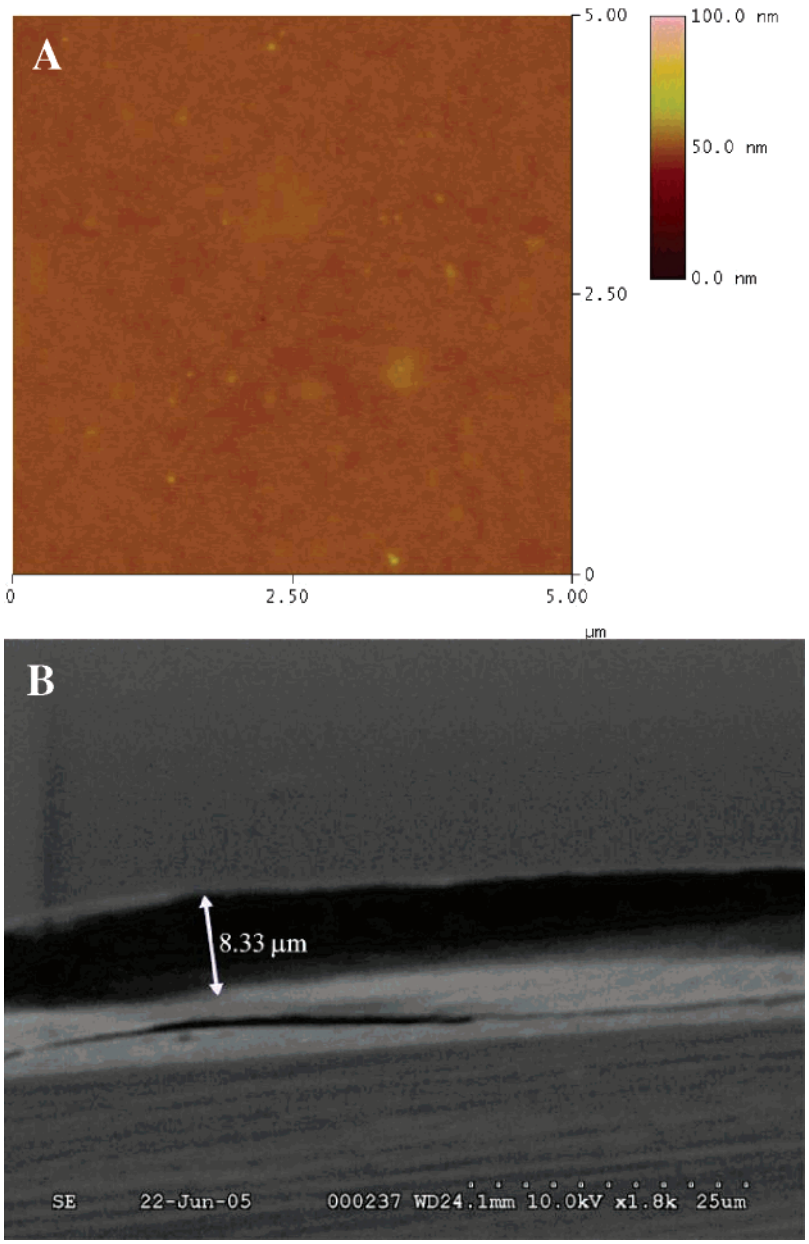

Figure 8. AFM (tapping mode with a Si tip) (5 μm $\times$ 5 μm) of GC electrode modified with two Nafion protective layers (A). SEM cross-section analysis of the thickness of Nafion (B).

thesis of reduced ascorbic acid in the presence of colloidal Pt. In the presence of the photoreaction, Pt^{2+} is reduced as follows:[20]

$$\mathrm{ZnP} + h\nu \rightarrow \mathrm{ZnP^*}$$

$$\mathrm{ZnP^*} + \mathrm{ED} \rightarrow \mathrm{ZnP^{-\bullet}} + \mathrm{ED_{ox}}$$

$$2\mathrm{ZnP^{-\bullet}} + \mathrm{Pt^{2+}} \rightarrow 2\mathrm{ZnP} + \mathrm{Pt^{o}}$$

Absorption of visible or UV light by the Zn porphyrin (ZnP) generates excited triplet $\pi-\pi^*$ state, ZnP*, which is rapidly reduced by ascorbic acid as an ED. The further reduction of the metal regenerates ZnP, which again becomes available to absorb light and initiate another photochemical cycle. It should be noted that seeding and autocatalytic reduction of platinum salts in aqueous solution using ascorbic acid as the reductant leads to dendritic metal nanostructures.[20]

RESULT AND DISCUSSION

General Characterization. TEM images of Pt nanoparticles prepared by chemical reduction of H_2PtCl_6 by ascorbic acid are shown in Figure 1A. The resulting particles were large (80−100 nm) with a broad particle size distribution. The formation of Pt nanoparticles was prevented by adding Zn porphyrin in the mixture of H_2PtCl_6 and ascorbic acid in the absence of light (Figure 1B). Extensive examination of many spots of the sample showed only a few dark spots consisting of carbon as confirmed by the EDX analysis. Panels C and D of Figure 1 (two different magnifications) show Pt−Zn porphyrin nanocomposites, products of the photocatalytic reaction. The formation of the nanocomposites occurred only when the solution consisting of Zn porphyrin, H_2PtCl_6, and ascorbic acid was irradiated with light. The resulting composite exhibited a spongelike structure with very small Pt

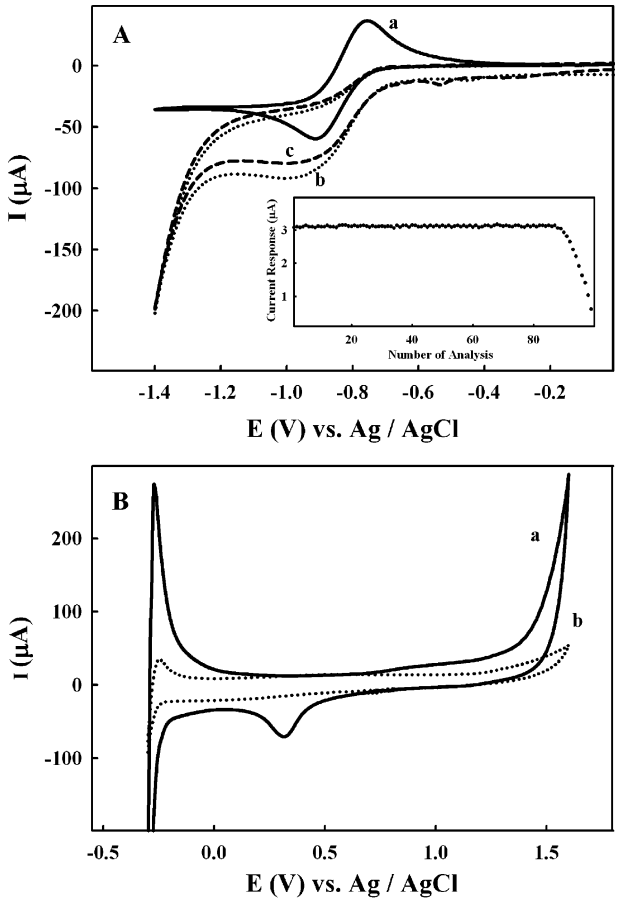

Figure 9. Reproducibility of the signal upon 100 consecutive analyses. (A) Cyclic voltammetry response before addition of the analyte (curve a), after first cycle upon addition of 2 mM $CHCl_3$ (curve b), and after 100 cycles with the analyte (curve c). The inset shows the amperommetric response of 100 analyses of 4 μM $CHCl_3$. (B) Cyclic voltammograms of Pt−Zn porphyrin nanocomposite after 1st (a) and 100th (b) cycle in 1.0 M H_2SO_4, scan rate 0.05 V/s.

nanoparticles (average size of 3.5 nm in diameter), embedded inside the structure (Figure 1D).

The SEM micrographs of the GC electrode modified with Zn porphyrin show that the smooth layer of Zn porphyrin was cracked due to the drying procedure (Figure 2A). When the reaction mixture (Zn porphyrin, H_2PtCl_6, and ascorbic acid) was kept in the dark, only a discontinuous Zn porphyrin layer was observed with no evidence of Pt nanoparticle formation (Figure 2B). When the reaction solution was exposed to light, Pt−Zn porphyrin nanocomposites were formed (Figure 2C), and SEM imaging was corroborated by AFM imaging of the GC electrode modified with the Pt−Zn porphyrin nanocomposite (Figure 2D).

UV−Visible/Fluorescence Characterization. Platinum nanoparticles were formed by chemical reduction due to the presence of ascorbic acid and H_2PtCl_6. Figure 3A shows the UV−visible absorbance during the reduction of Pt salt by ascorbic acid. The characteristic peak of H_2PtCl_6 at 280 nm decreased with time, whereas the background absorbance intensity increased due to the formation of large Pt nanoparticles. The slightly blackish precipitation of Pt colloids was usually observed after 20 min of the experiment. UV−visible spectra during the formation of Pt−Zn porphyrin nanocomposites are shown in Figure 3B. Characteristic peaks of porphyrin at 430 nm or the Soret band decreased significantly, and the peak at 570 nm almost disappeared after 10 min of light irradiation, while the background absorbance intensity increased drastically. The decrease of the characteristic 280-nm peak of the Pt salt was masked by the nanocomposite formed and could not be observed. The inset in Figure 3B shows the effect of light irradiation of the solution containing Zn porphyrin, H_2PtCl_6, and ascorbic acid on their fluorescence spectra.[24] The decrease in the fluorescence emission (excitation 400 nm) of the solution exposed to the light was pronounced.

Raman Spectroscopy. As a test model, Raman spectroscopy of chlorobenzene and the product resulting from the electrochemical reduction was studied. All solutions including the starting chlorobenzene were 2 mM in 0.1 M TBAP/ACN. Figure 4 shows the Raman spectra of chlorobenzene, benzene, the product of the electrochemical reduction, and 0.1 M TBAP/ACN as the background. Both benzene and the reduced product did not exhibit the Raman bands at 195, 290, 416, and 703 cm^{-1}, a Raman characteristic of chlorobenzene. In addition, in the high-frequency region of 800−1400 cm^{-1}, both benzene and the reduced product did not exhibit the Raman bands at 1002, 1022, and 1082 cm^{-1}, a Raman characteristic of chlorobenzene. The characteristic Raman peak for benzene at 991 cm^{-1} was also observed with the reduced product. Such results confirmed the dehalogenation of chlorobenzene by the nanocomposite-modified electrode.

Electrochemical Characterization. Figure 5 shows the CV characteristics of three different electrodes: bare GC/Nafion with a minimal background (a), Zn porphyrin/GC/Nafion (b), and Pt−Zn porphyrin nanocomposite/Nafion (c) in 0.1 M TBAP/ACN solution at 0.05 V/s in the potential range 1.6 to −1.5 V. For Zn porphyrin/GC/Nafion (curve b), two well-known one-electron porphyrin ring oxidation peaks[23,25] (eq 1) were observed with $E_{1/2}$ (1) = 0.505 V and $E_{1/2}$ (2) = 1.065 V, respectively, where $E_{1/2} = (E_{pa} + E_{pc})/2$. The one-electron porphyrin reduction[23,26] at −0.920 V versus Ag/AgCl (eq 2) peak was broad and not reversible (Table 1).

$$[ZnP] - e^- \leftrightarrow [ZnP]^{+\bullet} - e^- \leftrightarrow [ZnP]^{2+} \quad (1)$$

$$[ZnP] + e^- \leftrightarrow [ZnP]^- \quad (2)$$

The cyclic voltammogram of Pt−Zn porphyrin nanocomposite-modified GC electrode (curve c) exhibited well-defined and reversible Zn(I)/Zn(II) redox behavior with $E_{1/2} = -0.750$ V versus Ag/AgCl and peak-to-peak separation of 170 mV. Thus, in the region relevant for organohalide detection, Pt−Zn porphyrin nanocomposites displayed better reversibility, faster and more efficient electron transfer compared with only the Zn porphyrin-modified GC (Figure 7). Due to the presence of Pt nanoparticles, the porphyrin electroactivity in the positive potential range (one-electron porphyrin ring oxidation peaks) was less pronounced with E_{pa} (1) = 0.445 V and E_{pa} (2) = 1.085 V.

Figure 6 represents the voltammetric responses of 2 mM $CHCl_3$ in 0.1 M TBAP/ACN solution of three different electrode

(22) Ramachandraiah, G.; Bedioui, F.; Devynck, J.; Serar, M.; Bied-Charreton, C. *J. Electroanal. Chem.* **1991**, *319*, 395.
(23) Kadish, K. M.; Morrison, M. M. *Bioinorg. Chem.* **1977**, *7*, 107.
(24) Imahori, H.; Kashiwagi, Y.; Hanada, T.; Endo, Y.; Nishimura, Y.; Yamazaki, I.; Fukuzumi, S. *J. Mater. Chem.* **2003**, *13* (12), 2890.
(25) Fajer, J.; Borg, D. C.; Forman, A.; Dolphin, D.; Felton, R. H. *J. Am. Chem. Soc.* **1970**, *92*, 3451.
(26) Clack, D. W.; Hush, N. S. *J. Am. Chem. Soc.* **1965**, *87*, 4238.

materials: (A) Zn porphyrin/GC/Nafion, (B) Zn porphyrin, H_2PtCl_6, and ascorbic acid-dark conditions, and (C) Pt−Zn porphyrin nanocomposites/Nafion (light-irradiated Zn porphyrin, H_2PtCl_6, and ascorbic acid). The largest response to the analyte was given by GC modified with Pt−Zn porphyrin nanocomposites. To confirm the synergistic effect of Pt−Zn porphyrin nanocomposites, separately prepared Pt nanoparticles (2−3 nm) by the standard chemical reduction procedure[21] were mixed with an appropriate concentration of Zn porphyrin. The CV illustrated only a broad reduction wave, and the response to the added analyte was not comparable with Pt_o−Zn porphyrin nanocomposites prepared in situ (figure not shown).

The mechanism of the dehalogenation of organohalides (RX) by ZnTPP(II) can be described as follows:[16,22]

$$\mathrm{ZnTPP(II)} + e^- \rightarrow [\mathrm{ZnTPP(I)}]^{-\bullet}$$

$$[\mathrm{ZnTPP(I)}]^{-\bullet} + \mathrm{RX}_2 \rightarrow [\mathrm{ZnTPP(II)}] + \mathrm{RX}^{\bullet} + \mathrm{X}^-$$

$$[\mathrm{ZnTPP(I)}]^{-\bullet} + \mathrm{RX}^{\bullet} \rightarrow \mathrm{ZnTPP(II)} + \mathrm{RX}^-$$

$$\mathrm{RX}^{\bullet} \rightarrow \mathrm{alkene} + \mathrm{X}^-$$

where $RX^{\bullet}$ and RX^- are the two organometallic intermediates and X^- is the halide ion.

At least a 10-fold improvement in the amperometric response (2.2−500 μM chloroform) was observed for the GC electrode modified with Pt−Zn porphyrin nanocomposites/Nafion compared with the Zn porphyrin/Nafion-modified counterpart. Calibration curves were then established for chloroform, carbon tetrachloride, hexachlorobenzene, chlorobenzene, and pentachlorophenol, which were reduced at −1.0 V, using the same Pt−Zn porphyrin nanocomposite-modified GC electrode (Figure 7). The five organohalides could be determined from a common calibration curve (linear range from 500 nM to 8 μM, $R^2 = 0.9940$), which indicated the potential of this sensor to provide a general-purpose organohalide sensor. Such a result also implied that the dehalogenation step was not influenced by the chemical structure of the target analyte, in agreement with the results obtained by Dobson and Saini.[14] The detection limit (S/N = 3) was 500 nM, corresponding to 50−200 ppb, for the five organohalides examined. It should be noted that for a modified electrode consisting of a graphite coil covered with adsorbed cobalt porphyrin the detection limits were compound dependent; 500 nM, 10−20 μM and 30 μM for haloalkanes, haloalkenes and haloarenes, respectively.[14] Smaller responses were observed at the higher concentration of chlorobenzene, hexachlorobenzene, and pentachlorophenol compared to chloroform and carbon tetrachloride, and this effect was likely due to the relative insolubility of these compounds in the electrolyte solution.

Reproducibility and Stability of the Modified Electrode. The reproducibility of Pt−Zn porphyrin complex nanoparticle-modified GC electrode, poised at −1.0 V versus Ag/AgCl, was examined by performing 100 consecutive measurements at 4 μM chloroform. To obtain the desired reproducibility and stability of the modified electrodes, the application of two protective layers of Nafion was required. AFM imaging confirmed continuity and uniformity of the double Nafion protective layers without pores or cracks (Figure 8A). SEM cross-section analysis (Figure 8B) revealed that the overall thickness of the two Nafion layers was 8−9 μm, in good agreement with the estimated values reported in the literature.[27,28] The reproducibility results upon the optimization using the two layers of Nafion are shown in Figure 9A (inset), and the response was invariant for 80 measurements. Figure 9A shows cyclic voltammetry response before the addition of the analyte (curve a), after the first cycle upon addition of 2 mM $CHCl_3$ (curve b) and after 100 cycles with the analyte (curve c). Figure 9B shows cyclic voltammograms of the Pt−Zn porphyrin nanocomposite after the 1st and 100th cycle in 1.0 M H_2SO_4, scan rate 0.05 V/s. The CV characteristics of Pt (H_{ads}, platinum oxide formation and its reduction) were clearly visible during the cycling (curve a). After 100 repeated analyses (curve b), the peak height and shape changed, and the CV characteristics of Pt almost disappeared. The catalytic significance of Pt nanoparticles in Zn porphyrin nanostructures is a subject of future study, and it has been noted that the platinum particles combined with the porphyrin nanotube act as a catalytic device for photocatalytic water reduction.[29] When stored at room temperature, the modified electrode was stable up to 30 days without compromising its catalytic activity.

In brief, platinum−porphyrin nanocomposites have been synthesized, characterized, and used as sensing materials for analysis of organohalides. Our study confirms the potentiality of such nanocomposites in the reductive dehalogenation process of five common organohalides. The detection limit is sufficient to satisfy regulatory requirements, and the nanocomposite-modified electrode can be used for repeated analyses without fouling or compromising its catalytic activity. The sensor can be coupled with an upstream scheme such as liquid chromatography or capillary electrophoresis for analysis of a mixture of organohalides in environmental samples. Analysis of organohalides using contaminated samples and the validation of results obtained by the nanocomposite-modified electrode are in progress in our laboratories and will be reported in due course. Besides their potential as electrode materials for screening organohalides, such nanocomposites also offer future prospects for transformation of organohalides in the environment. Although Zn porphyrin exhibits very high catalytic activity toward organohalides as illustrated in this study and recently reported by Wiyaratn et al.,[30] the synthesis and catalytic activity of nanocomposites derived from other metal porphyrins including Cu porphyrin is a subject of future endeavor.

ACKNOWLEDGMENT

The authors thank D. Wang of the Institute of Chemical and Environmental Technology (ICPET), National Research Council Canada, Ottawa, ON, Canada for performing TEM experiments. W.W. has received a Ph.D. Scholarship from the Royal Golden Jubilee Project of the Thailand Research Fund and NRC Canada, Biotechnology Research Institute.

Received for review June 1, 2005. Accepted July 3, 2005.

AC0509612

(27) Brown, R. S.; Luong, J. H. T. *Anal. Chim. Acta* **1995**, *310*, 419.
(28) Oyama, N.; Ohsaka, T.; Ushirogouchi, T.; Sanpei, S.; Nakamura, S. *Bull. Chem. Soc. Jpn.* **1988**, *61*, 3103.
(29) Wang, Z.; Medforth, C. J.; Shelnutt, J. A. *J. Am. Chem. Soc.* **2004**, *126*, 16720.
(30) Wiyaratn, W.; Somasundrum, M.; Surareungchai, W. *Electroanalysis* **2003**, *130*, 626.